Use of an Altered Sugar-Nucleotide To Unmask the Transition State for α(2→6) Sialyltransferase†

Michael Bruner and Benjamin A. Horenstein*

Department of Chemistry, University of Florida, Gainesville, Florida 32611

Received June 28, 1999; Revised Manuscript Received November 17, 1999

ABSTRACT: Rat liver α(2→6) sialyltransferase catalyzes the formation of a glycosidic bond between *N*-acetylneuraminic acid and the 6-hydroxyl group of a galactose residue at the nonreducing terminus of an oligosaccharide. This reaction has been investigated through the use of the novel sugar-nucleotide donor substrate UMP-NeuAc. A series of UMP-NeuAc radioisotopomers were prepared by chemical deamination of the corresponding CMP-NeuAc precursors. Kinetic isotope effects (KIEs) on *V/K* were measured using mixtures of radiolabeled UMP-NeuAc's as the donor substrate and *N*-acetyllactosamine as the acceptor. The secondary β-^{2}H KIE was 1.218 ± 0.010, and the primary ^{14}C KIE was 1.030 ± 0.010. A large inverse ^{3}H binding isotope effect of 0.944 ± 0.010 was measured at the terminal carbon of the NeuAc glycerol side chain. These KIEs observed using UMP-NeuAc are much larger than those previously measured with CMP-NeuAc [Bruner, M., and Horenstein, B. A. (1998) *Biochemistry 37*, 289−297]. Solvent deuterium isotope effects of 1.3 and 2.6 on *V/K* and V_{max} were observed with CMP-NeuAc as the donor, and it is revealing that these isotope effects vanished with use of the slow donor substrate UMP-NeuAc. Bell-shaped pH versus rate profiles were observed for V_{max} (pK_a values = 5.5, 9.0) and $V/K_{UMP-NeuAc}$ (p$K_a$values = 6.2, 9.0). The results are considered in terms of a mechanism involving an isotopically sensitive conformational change which is independent of the glycosyl transfer step. The isotope effects reveal that the enzyme-bound transition state bears considerable charge on the *N*-acetylneuraminic acid residue, and this and other features of this mechanism provide new directions for sialyltransferase inhibitor design.

Oligosaccharides and polysaccharides serve diverse roles in nature including structure, energy storage, and information (*1*). These compounds are biosynthesized by glycosyltransferases, which catalyze glycoside formation by facilitating a net attack of a saccharide hydroxyl group at the anomeric carbon of a sugar-nucleotide. Glycosyltransferases are related to glycosidases because these two groups of enzymes transfer a saccharide glycon between donor and acceptor nucleophiles as is shown in Scheme 1.

Glycosidases cleave a stable glycon−OR bond (R is another sugar for natural substrates) and transfer the glycon to water. Glycosyltransferases cleave the bond to a phosphate leaving group, and transfer the saccharide glycon to a hydroxyl group of another saccharide unit with high regioselectivity. Water must be effectively excluded from the active site to prevent hydrolysis of the sugar-nucleotide. For a variety of reasons, mechanistic studies of glycosyltransferases and glycosyl phosphates have lagged far behind those devoted to glycosidases and alkyl and sugar acetals (*2*−*4*). With this in mind, we are interested in defining glycosyltransferase mechanisms, the chemistry and enzymology of the glycosyl−phosphate bond, and ultimately the development of glycosyltransferase inhibitors.

Scheme 1

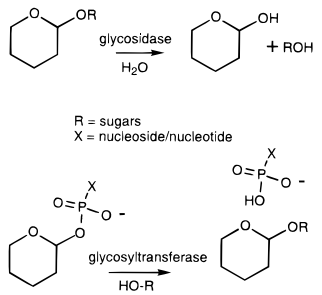

Sialyltransferases catalyze the transfer of NeuAc[1] from CMP-NeuAc, **1**, with inversion of configuration to acceptor hydroxyl groups at or near the nonreducing termini of oligosaccharide chains of glycoproteins and glycolipids as is shown in Scheme 2(*5*). Sialyltransferases are widely distributed, being found in higher eukaryotes, bacteria, and viruses, but apparently not in simple eukaryotes such as yeasts (*6*−*9*). Cell-surface sialic acids affect the gross physical−chemical properties of a cell, and they also comprise recognition sites for many different macromolecular binding interactions that are part of cell adhesion, with

†Support of this work by the National Science Foundation (CAREER award Grant MCB-9501866) and the University of Florida Division of Sponsored Research is gratefully acknowledged.

* Address correspondence to this author. Phone: (352) 392-9859, FAX: (352) 846-2095, E-Mail: horen@chem.ufl.edu.

[1] Abbreviations: C_f, forward commitment to catalysis; CMP-NeuAc, cytidine monophosphate glycoside of *N*-acetylneuraminic acid; UMP-NeuAc, uridine monophosphate glycoside of *N*-acetylneuraminic acid; KIE, kinetic isotope effect; LacNAc, *N*-acetyllactosamine; NeuAc, *N*-acetylneuraminic acid; ST, sialyltransferase.

10.1021/bi991474h CCC: $19.00
Published on Web 02/12/2000

Scheme 2

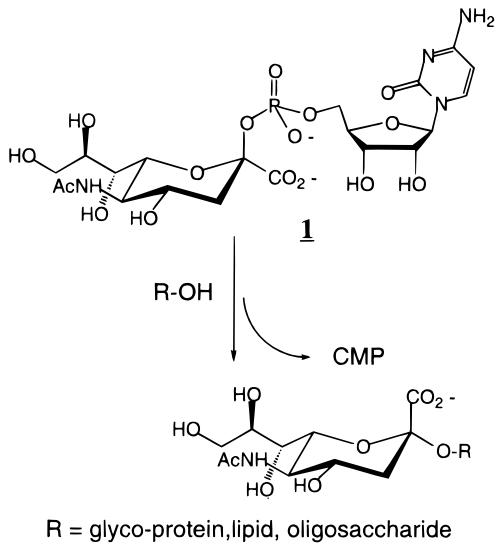

functions that include pathogen−host binding interactions, inflammation, and metastasis (*10*−*14*).

One of the best characterized sialyltransferases is the α-(2→6) enzyme from rat liver. Obtained as the lumenal C-terminal catalytic domain due to proteolysis during isolation, the enzyme is N-glycosylated with a molecular mass of ∼41 kDa for the protein (*15*, *16*). The enzyme has a broad acceptor specificity, but prefers sialylation of terminal Gal-β(1→4)-GlcNAc residues (*17*−*20*). Some minor modifications in the NeuAc ring of the donor substrate CMP-NeuAc are tolerated, but the preference for an unmodified cytidine nucleotide is strong (*21*−*23*).

One of the interesting features of sialyltransferases is the unique structure and reactivity of the donor substrate CMP-NeuAc, **1** (*24*). This substrate has a carboxylate group immediately adjacent to the anomeric carbon, differentiating it from aldoses and ketoses which have hydrogen or a hydroxymethyl group bonded to the anomeric carbon. Experimental and theoretical investigation of the solution chemistry of CMP-NeuAc has revealed that its acid-catalyzed solvolysis proceeds by an extremely late transition state, with no significant nucleophilic participation by solvent or the carboxylate group (*25*, *26*). After the transition state, short-lived oxocarbenium ion intermediates are formed that are likely stabilized by intramolecular ion-pairing with the carboxylate group (*27*, *28*). The kinetic isotope effects for solvolysis of CMP-NeuAc are considerably different than the kinetic isotope effects for the sialyltransferase-catalyzed transfer reaction (*29*). The β-secondary dideuterium isotope effect for solvolysis was 1.276, while it was 1.044 for the sialyltransferase reaction. The primary ^{14}C KIE was also diminished, decreasing from 1.030 for solvolysis to 1.000 for the sialyltransferase-catalyzed reaction of CMP-NeuAc. A comparison of these KIEs suggests that the mechanism for the enzymatic transfer of NeuAc is considerably different than in solution, or that additional kinetic complexity of the sialyltransferase reaction is masking the true intrinsic value of the KIE.

Here we present work that resolves this question and further defines the kinetic and chemical mechanism of sialyltransferase. We report a practical synthesis of the nonnatural sugar-nucleotide UMP-NeuAc, and its characterization as a slow substrate for α(2→6) sialyltransferase. UMP-NeuAc affords simplified pH−rate profiles and unmasks large kinetic isotope effects. Solvent deuterium isotope effects on V_{max} and $V/K_{sugar-nucleotide}$ were measured and provide evidence for a multistep mechanism for sialyltransfer.

MATERIALS AND METHODS

Materials. Buffers and reagents were purchased from Sigma and Fisher. NANA aldolase was purchased from Shinko American. Rat liver α(2→6) sialyltransferase was purchased from Sigma or Boehringer. *N*-Acetylmannosamine isotopomers ([6-^{3}H] and [1-^{14}C-*N*-*acetyl*]) and sodium pyruvate ([1-^{14}C]) were purchased from New England Nuclear and Moravek. D_2O (99.9% D) used in the solvent isotope effect studies was obtained from Cambridge Isotope Laboratories, Inc. Cytidine and uridine triphosphates (CTP and UTP) were purchased from Sigma as the disodium salt with 2.5 equiv of hydration. Liquid scintillation fluid (ScintiSafe 30%) was purchased from Fisher. The *E. coli* expression plasmid pWV200B harboring the *E. coli* CMP-NeuAc synthase gene was a gift from Dr. W. F. Vann at the National Institutes of Health. CMP-NeuAc synthase was purified from *E. coli* JM105 following the published protocol and was judged 90−95% pure based on SDS−PAGE analysis (*30*). Amberlite IR120-H^+ form resin which was used for desalting CMP-NeuAc and UMP-NeuAc was first washed with 95% ethanol and then washed extensively with deionized water.

Instrumental. HPLC separations were performed on a MonoQ HR10/10 anion exchange column (Pharmacia) monitored at 260 nm. Liquid scintillation counting was performed using a Packard 1600 TR instrument which dumped data to a floppy disk for subsequent analysis on a personal computer. An Orion Sure-Flow pH probe was used for all pH measurements. A Rainin-Dynamax fraction collector (model FC-1) was used to collect eluent samples from the HPLC for kinetic isotope effect experiments.

Synthesis of UMP-NeuAc Isotopomers. CMP-NeuAc isotopomers were prepared and purified as previously described (*25*, *29*) and subsequently deaminated to the corresponding UMP-NeuAc isotopomer with nitrous acid by the following general procedure. The appropriate CMP-NeuAc isotopomer (2−10 μCi/reaction; 16−50 μCi/μmol specific activity for ^{14}C and 10 Ci/mmol specific activity for ^{3}H) was dissolved in 50−500 μL of a 1 N $NaNO_2$ solution adjusted to pH 4−5 with 1 N HCl (10−50 μL) and allowed to react at 4 °C. Evolution of gas, presumably N_2, was noted after acidification of the reaction mixture. Deamination reactions were monitored by anion exchange HPLC (100 mM NH_4HCO_3, 15% methanol, pH 8.0, 2 mL/min) by following the conversion of CMP-NeuAc (retention time, 13.5 min) to UMP-NeuAc (retention time, 17.5 min). Reactions were allowed to proceed for 48 h at 4 °C, with the pH being maintained in the range of 4−5 by manual addition of 1 N HCl as required. UMP-NeuAc was purified from the reaction mixture by anion-exchange chromatography (50 mM NH_4HCO_3, 15% methanol, pH 8.0, 2 mL/min). The collected UMP-NeuAc fractions were desalted with Amberlite IR120-H^+ cation-exchange resin as described for CMP-NeuAc (*25*).

General KIE Methodology. Kinetic isotope effects on α-(2→6) sialyltransferase reactions were measured by the dual-label competitive method (*31*, *32*). Experiments employed

ca. 100 000 cpm each of the appropriate ^{3}H- and ^{14}C-labeled UMP-NeuAc isotopomers. In a typical experiment, a master mixture containing a given ^{3}H/^{14}C-labeled UMP-NeuAc isotopomeric pair and 20 mM LacNAc in 40 mM cacodylate buffer (0.2 mg/mL BSA, 0.2% Triton CF-54, pH 7.0) was prepared. Aliquots were withdrawn from this master for individual reactions and for measurement of the control reference ^{3}H/^{14}C ratio at 0% conversion. Reactions were initiated by the addition of the appropriate amount of enzyme to 50−100 μL reaction mixtures to give 40−60% (*33*) conversion in <45 min at 37 °C. After 40−60% conversion, unreacted substrate was isolated by anion-exchange HPLC (100 mM NH_4HCO_3, 15% methanol, pH 8.0, 2 mL/min) and collected directly into 20 mL glass scintillation vials (2 mL fractions). Care was taken to collect the entire UMP-NeuAc peak. The percent conversion was determined from the ratios of the UMP-NeuAc and UMP peaks in the HPLC chromatogram. The initial ^{3}H/^{14}C ratio was obtained in triplicate by injecting aliquots of the master mixture of labeled UMP-NeuAc on the MonoQ column and recollecting the entire UMP-NeuAc peak. The ^{3}H/^{14}C ratios for collected fractions were determined by dual-channel liquid scintillation counting (channel A, 0−12 keV; channel B, 12−80 keV) with each tube being counted for 10 min, and all tubes were cycled through the counter 6−10 times. The internal ^{133}Ba source was used to estimate the quench parameter for each tube, which varied by ±1%. Triplicate samples of [^{14}C]CMP-NeuAc were used to determine the ratio of ^{14}C counts in channels A and B (A:B^{14}). Since ^{3}H is only detected in channel A, the ^{3}H/^{14}C ratio can be calculated with eq 1. The observed KIE was calculated with eq 2 or 3. The observed KIE was then corrected for fractional conversion using eq 4 (*34*). The reported value and error of a KIE represents the mean and standard deviation of three separate KIE reactions taken over 6−10 cycles through the liquid scintillation counter:

$$^3H/^{14}C = [\text{cpm } A - \text{cpm } B*(A{:}B^{14})]/[\text{cpm } B + \text{cpm } B*(A{:}B^{14})] \quad (1)$$

$$^3H\ \text{KIE}_{\text{observed}} = (^3H/^{14}C)_0/(^3H/^{14}C)_{t1/2} \quad (2)$$

$$^{14}C\ \text{KIE}_{\text{observed}} = (^{14}C/^3H)_0/(^{14}C/^3H)_{t1/2} \quad (3)$$

$$\text{KIE}_{\text{corrected}} = \ln(1-f)/\ln[(1-f)\text{KIE}_{\text{observed}}] \quad (4)$$

where f = fraction of reaction.

The above KIE method was previously used to measure KIEs for sialyltransferase with CMP-NeuAc as the glycosyl donor (*29*). Control experiments established that the HPLC methodology does not introduce artifactual isotopic fractionation (*25*).

Kinetic Methodology. All kinetic experiments were performed at 37 °C. Reaction rates were measured by quantifying the radiolabeled product (sialyl-LacNAc) isolated by chromatographing reaction mixture aliquots on Dowex mini-columns, which retain unreacted sugar-nucleotide but readily pass sialyl-LacNAc (*17*). Time point aliquots (20−30 μL) were removed from reaction mixtures and quenched in 500 μL of ice-cold 5 mM P_i buffer at pH 6.8. Aliquots of 500 μL were withdrawn and applied to columns (0.5 × 4 cm) of Dowex-1 × 2-200 anion-exchange resin (P_i form). A volume of 3.5 mL of 5 mM P_i buffer was applied to each column to elute the product, which was collected directly into liquid scintillation vials for counting.

Kinetic Parameters for UMP-NeuAc. The kinetic constants for sialyltransferase with UMP-NeuAc and LacNAc as the donor−acceptor pair were estimated by varying the UMP-NeuAc concentration while holding LacNAc at a high near-saturating concentration, and by varying the LacNAc concentration while holding UMP-NeuAc at a near-saturating concentration. Reaction mixture volumes were 67 μL, and the buffer was 40 mM sodium cacodylate, 0.2 mg/mL BSA, 0.2% Triton CF-54, pH 7.5. Each reaction contained 64 000 cpm of [9-^{3}H]-UMP-NeuAc diluted to the required specific activity. Reaction mixtures with LacNAc concentration held fixed at 40 mM and UMP-NeuAc concentrations of 0.1, 0.2, 0.5, 1.0, 2.0, and 5.0 mM were prepared. The reactions were initiated by the addition of 4.3 milliunits of enzyme (8 units/mg). Aliquots of 20 μL were removed at 5, 10, and 15 min, and the product was quantified using Dowex mini-columns. Another series of reaction mixtures were prepared with UMP-NeuAc concentration held fixed at 2 mM and LacNAc concentrations of 20, 4, 2, 1.33, and 1 mM. These reactions were initiated by addition of 5.7−12.9 milliunits of sialyltransferase. Aliquots of 30 μL were removed at 10 and 20 min and were fractionated on Dowex mini-columns. The initial velocity data were fit to eq 5 for a sequential kinetic mechanism:

$$v = \frac{V_{\max}[\text{A}][\text{B}]}{K_{\text{A}}[\text{B}] + K_{\text{B}}[\text{A}] + [\text{A}][\text{B}] + K_{i\text{A}}K_{\text{B}}} \quad (5)$$

pH vs Rate with CMP-NeuAc. The pH behavior of V_{max} for sialyltransferase was estimated by holding [CMP-NeuAc] and [LacNAc] at 10K_m values. Stock 2× reaction buffers of either 800 mM Tris/Bis-Tris (pH 6−9) or 800 mM sodium acetate (pH 4−6) were prepared at 37 °C. Each of these buffers also contained 20 mM LacNAc. A second stock solution containing 700 μM [1-^{14}C]-CMP-NeuAc (60 000 cpm/reaction, 1.3 mCi/mmol) was prepared. The CMP-NeuAc stock (30 μL) and the LacNAc stock (30 μL) at the appropriate pH were combined and incubated briefly at 37 °C before initiation of the reaction by addition of 0.45 milliunit of sialyltransferase. Aliquots of 20 μL were withdrawn at 2, 4, and 6 min, and the product was quantified with the Dowex column methodology described above. Control reactions were performed at the pH extremes to account for background hydrolysis, which was only significant for pH values <5. Enzymatic reaction rates at these pH values were corrected by subtraction of the background hydrolysis rate. The pH behavior of $V/K_{\text{CMP-NeuAc}}$ was estimated by the same procedure and with the same buffer systems described above. In these experiments, [LacNAc] was held at 10K_m, and [CMP-NeuAc] was 44 nM, well below its K_m. In all experiments, sialyltransferase was found to be stable at the pH extremes over the time frame employed based on no observed loss in activity.

pH vs Rate with UMP-NeuAc. The pH behavior of V_{max} for sialyltransferase was estimated by holding [UMP-NeuAc] and [LacNAc] at approximately 2K_m and 10K_m values. The stock 2× buffers consisted of sodium acetate, sodium cacodylate, Bis-Tris propane, and CHES at 250 mM each, plus 40 mM LacNAc, 2 mg/mL BSA, and 0.2% Triton CF-

54. Aliquots of the buffer were adjusted to the required pH at 37 °C before being brought to final volume. Enzyme was added (1 milliunit for pH 6−8.5; 1.2 milliunits for pH 5−6 and 8.5−10) to each buffer/LacNAc mixture (30 μL) and incubated at 37 °C, 1 min. Reactions (final volume = 65 μL) were initiated by addition of an equal volume (30 μL) of [9-^{3}H]-UMP-NeuAc (4 mM, 120 000 cpm/reaction, 0.69 μCi/μmol). Aliquots of 20 μL were removed at 8, 16, and 24 min, and the product was quantified on Dowex mini-columns. Reactions were run in the pH range 4.95−9.7 with control reactions at the pH extremes to account and correct for any background hydrolysis of substrate. The pH behavior of $V/K_{UMP-NeuAc}$ was estimated by the same procedure and with the same buffer systems described above. In these experiments, [LacNAc] was held at $10K_m$, and [UMP-NeuAc] was 300 nM, well below its estimated K_m. The data were fit to eq 6 in which v = the observed velocity at a given pH, the constant C represents the value of V_{max} or V/K that would be observed if 100% of the enzyme were in the correct protonation state, and K_{a1} and K_{a2} are the acid dissociation constants of two residues on the acid and basic limbs of the profile:

$$\log v = \log\left(\frac{C}{1 + \frac{[H^+]}{K_{a1}} + \frac{K_{a2}}{[H^+]}}\right) \quad (6)$$

Solvent Isotope Effects. For measurement of the solvent deuterium isotope effect on V_{max} with UMP-NeuAc as the donor substrate, a stock solution containing 4 mM [9-^{3}H]-UMP-NeuAc (40 000 cpm/reaction, 0.69 μCi/μmol) and 40 mM LacNAc was prepared in 250 mM Bis-Tris propane buffer, 0.2 mg/mL BSA, 0.2% Triton CF-54, pH 7.8. Half of the reaction mixture was retained for the reaction in H_2O while the other half was concentrated to dryness on a rotary evaporator equipped with a mechanical vacuum pump. The residue was dissolved and reconcentrated 2 times in D_2O, and then brought to the original volume in 99.9% D_2O. The pD of the D_2O mixture was determined to be 7.6 after exchange in D_2O (pD = pH meter reading + 0.4) (*35*). Reactions (60 μL) were preincubated at 37 °C for 1 min before being initiated by the addition of 5 μL (1.2 milliunits) of α(2→6) sialyltransferase. Aliquots of 20 μL were removed at 6, 12, and 18 min, and the product was quantified with Dowex mini-columns. The solvent deuterium isotope effect on $V/K_{UMP-NeuAc}$ was measured by the same procedure and in the same buffer system, but the final concentration of UMP-NeuAc was 0.3 μM in these experiments. Solvent deuterium isotope effects with CMP-NeuAc as the donor substrate were measured by the same procedure described above, but were obtained at pH 6.5 in 40 mM sodium cacodylate buffer containing 16 mM LacNAc, 0.2 mg/mL BSA, and 0.2% Triton CF-54. In the V_{max} experiments, the concentration of CMP-NeuAc was 500 μM; for V/K, the concentration was 11 μM. Control experiments for viscosity effects of D_2O at 37 °C were made by taking initial velocity measurements under V_{max} and V/K conditions in the presence and absence of 9% (v/v) glycerol (*36*, *37*).

RESULTS

Synthesis of UMP-NeuAc Isotopomers. The synthesis of the alternate sialyltransferase donor substrate uridine-5′-monophosphate neuraminic acid (UMP-NeuAc) was carried out by chemical deamination of CMP-NeuAc to afford the isotopomers identified in Table 1and Figure 1. The reaction proceeds with 50% conversion of CMP-NeuAc to UMP-NeuAc in 48 h with ∼10% hydrolysis of either sugar-nucleotide as indicated by HPLC. UMP-NeuAc obtained by this method was identical to UMP-NeuAc obtained by CMP-NeuAc synthase-catalyzed reaction of UTP and NeuAc on the basis of HPLC co-injection and ^{1}H NMR spectra (*29*). UMP-NeuAc was routinely obtained in 30−40% purified yield from CMP-NeuAc with 20−30% of starting CMP-NeuAc recovered. The remaining mass balance is accounted for by the hydrolysis products NeuAc, UMP, and CMP, which are cleanly separated from UMP-NeuAc by HPLC purification.

Table 1: UMP-NeuAc Isotopomers and Yields

isotopomer	% yield[a]
[9-^{3}H]	18
[2-^{14}C]	40
[(1-^{14}C)-*N-acetyl*]	28
[^{3}H-*N*−*acetyl*]	33
[^{3}H-*N-acetyl*; 3,3′-$^2H_2$]	38

[a] Yield is from CMP-NeuAc.

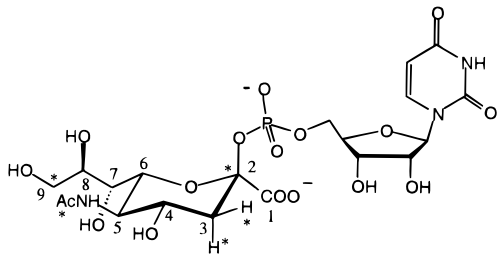

FIGURE 1: UMP-NeuAc isotopomers. The structure presents the numbering scheme for the NeuAc residue. Asterisks identify locations that are labeled.

Kinetic Constants and pH Dependence. The kinetic parameters for α(2→6) sialyltransferase using UMP-NeuAc and LacNAc as the donor−acceptor substrate pair were estimated at pH 7.5 and 37 °C. The K_m for UMP-NeuAc was 1.2 ± 0.1 mM, the K_m for LacNAc was 4.9 ± 0.3 mM, and the V_{max} was 1.8 μmol/(min·mg) with a corresponding k_{cat} of 1.2 s^{-1}. Relative to CMP-NeuAc, UMP-NeuAc is very weakly bound by sialyltransferase, and V_{max} is somewhat reduced, as will be discussed further below. The effect of pH on the kinetic parameters for sialyltransferase with CMP-NeuAc and UMP-NeuAc as donor substrate are presented in Figures 2 and 3. When CMP-NeuAc is used as the donor substrate, the pH profiles obtained are complex (Figure 2). On the acid limb, both the V and V/K profiles showed a limiting slope of 2 and an apparent pK_a near 5.3. The V_{max} profile reached an optimum near pH 6, and then decreased with an apparently nonintegral slope toward alkaline pH, whereas the V/K profile reached a maximum limiting plateau after the acid-side pK_a of ∼5.3. The pH profiles with the slow substrate UMP-NeuAc (Figure 3) were quite different from those discussed above. The bell-shaped data were well fit to eq 6 which describes a model which requires a single ionizable group in its unprotonated form, and another group in its protonated form. For the V_{max} plot, the pK_a values were 5.5 and 9.0 whereas for $V/K_{UMP-NeuAc}$ the values were 6.2 and 8.9.

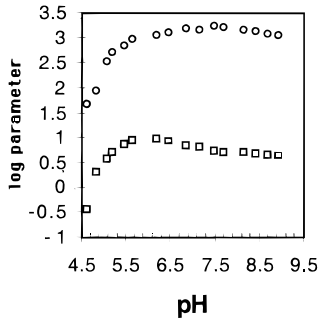

FIGURE 2: pH−rate profiles with CMP-NeuAc as donor substrate. The circles represent the experimental k_{cat}/K_m data, and the squares represent the k_{cat} data. Units are M^{-1} s^{-1} for k_{cat}/K_m and s^{-1} for k_{cat}.

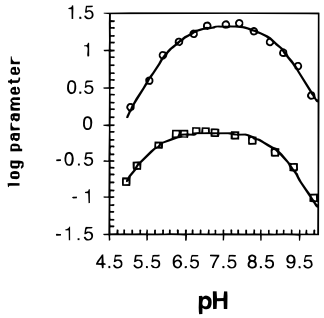

FIGURE 3: pH−rate profiles with UMP-NeuAc as donor substrate. The circles represent the experimental k_{cat}/K_m data, and the squares represent the k_{cat} data. Units are M^{-1} s^{-1} for k_{cat}/K_m and s^{-1} for k_{cat}, and the solid lines represent the fit of the data to eq 6.

Kinetic Isotope Effects with CMP-NeuAc and UMP-NeuAc. The kinetic isotope effect methodology used in this study utilized radiolabeled substrates, so the isotope effects are on the kinetic parameter *V/K (38)*. The *V/K* KIEs for the enzyme-catalyzed reaction with UMP-NeuAc were measured at pH 7 and 37 °C and are presented in Table 2. For comparison, the KIEs for the enzyme reaction with the natural donor substrate CMP-NeuAc and solvolysis of both CMP-NeuAc and UMP-NeuAc are provided.

A β-dideuterio KIE of 1.218 ± 0.010 was measured with UMP-NeuAc as the donor substrate and LacNAc as the acceptor substrate. The magnitude of this effect is close to that measured for the acid-catalyzed hydrolysis of CMP-NeuAc, and much greater than that measured for the enzyme reaction with the natural donor substrate CMP-NeuAc. A value of 1.28 ± 0.01 for the β-dideuterio isotope effect on the acid-catalyzed hydrolysis reaction of UMP-NeuAc was also measured, which is identical within experimental error to that measured for CMP-NeuAc. A primary ^{14}C KIE of 1.028 ± 0.010 was measured on the enzyme-catalyzed reaction with UMP-NeuAc, which is almost identical to that observed for the solvolysis reaction of CMP-NeuAc. A large ^{3}H inverse binding isotope effect of 0.944 ± 0.010 was measured at C9 of the C6−C9 glycerol tail of NeuAc. Finally, a control KIE of 1.005 ± 0.005 was measured for ^{3}H and ^{14}C labels positioned in the *N*-acetyl group of UMP-NeuAc. This control shows that the remote labels do not experience a KIE themselves.

Solvent Isotope Effects. The effects of solvent deuterium substitution on V_{max} and *V/K* for the altered donor substrate (UMP-NeuAc) were measured for α(2→6) sialyltransferase. In both cases, effects close to unity were measured. In contrast, CMP-NeuAc showed a solvent isotope effect of 1.3 on *V/K* and 2.6 on V_{max}. The isotope effects are apparently not related to the difference in viscosity of H_2O and D_2O (*36*) since control experiments with glycerol as an added viscogen failed to show measurable differences in velocity for *V/K* or V_{max}. The results for the substrate dependence of the solvent isotope effects are in counterpoint to those for the β-^{2}H and primary ^{14}C isotope effects. The observed solvent isotope effects are higher with the "fast" substrate CMP-NeuAc than they are with UMP-NeuAc. The KIEs for the isotope-labeled NeuAc are suppressed with CMP-NeuAc but are maximal with the "slow" substrate UMP-NeuAc.

DISCUSSION

The observed KIEs measured for sialyltransferase with the natural substrate CMP-NeuAc were very small. This indicated that one or more kinetic barriers other than the one for the chemical step were at least partially rate-limiting, resulting in a situation termed commitment to catalysis (*39*, *40*). Isotope trapping experiments revealed that when the acceptor oligosaccharide *N*-acetyllactosamine was held at its K_m value, the net rate for enzyme-bound CMP-NeuAc dissociation was equal to the net rate at which it proceeded forward to form product. This commitment factor of 1.0 allowed correction of the observed isotope effects, but the KIEs were still small when corrected for this factor (*29*) which lead us to consider that additional slow steps after binding remained unaccounted for. We synthesized UMP-NeuAc, **2**, to test this hypothesis. This analogue is identical to CMP-NeuAc except for interchange of an oxo group for the 4-amino group of the pyrimidine ring. UMP-NeuAc is bound more weakly to sialyltransferase than CMP-NeuAc, as indicated by its 30-fold higher K_m. The k_{cat} for UMP-NeuAc is 5 times lower than the k_{cat} for CMP-NeuAc; the increased barrier for the chemical step and the weaker binding of UMP-NeuAc provide the conditions that should lead to full expression of the kinetic isotope effects. The size of the isotope effects measured with UMP-NeuAc (Table 2) supports the idea that this has happened. The β-^{2}H isotope effect (1.22) is nearly as large as the 1.28 β-^{2}H isotope effects measured for solvolysis of either CMP-NeuAc or UMP-NeuAc. Further, the primary ^{14}C isotope effects for the sialyltransferase UMP-NeuAc reaction and solvolysis of CMP-NeuAc are identical (1.030). The β-^{2}H KIEs for the solvolysis reaction present a rough upper limit for the magnitude of the enzymatic KIE, and the observed similarity between the two sets of KIEs argues that the enzyme KIEs measured with UMP-NeuAc are intrinsic ones, or very nearly so.

Conformational Change on the Catalytic Cycle. The observed β-^{2}H isotope effect with UMP-NeuAc was 1.218, which is 10 times larger than the 1.022 isotope effect observed with CMP-NeuAc as the substrate and is 4.5 times larger than the CMP-NeuAc isotope effect when it was corrected for the slow CMP-NeuAc off-rate (*29*). The differences in sialyltransferase KIEs measured with CMP-NeuAc and UMP-NeuAc could be explained on the basis of additional kinetic complexity, or if the chemical nature of the transition states were different. Arguments that require significantly different transition states (and isotope effects) arising purely from differences in the intrinsic chemical reactivity of these two glycosyl donors are ruled out given

Table 2: Kinetic Isotope Effects for Sialyltransferase with UMP-NeuAc[a]

isotopomeric pair	type of KIE	$KIE_{UMP-NeuAc}$	$KIE_{CMP-NeuAc}$	solvolysis[b]
[1-^{3}H-*N*-acetyl; 3,3′-^{2}H$_2$], [1-^{14}C-*N-acetyl*]	β-secondary	1.218 ± 0.010	1.044 ± 0.007	1.276 ± 0.008, 1.28 ± 0.01[c]
[2-^{14}C], [1-^{3}H-*N-acetyl*]	primary ^{14}C	1.028 ± 0.010	1.000 ± 0.004	1.030 ± 0.005
[9-^{3}H], [1-^{14}C-*N-acetyl*]	binding	0.944 ± 0.010	0.984 ± 0.007	NA
[2-^{14}C], [9-^{3}H]	primary ^{14}C and binding	1.102 ± 0.012	NA	NA
[1-^{3}H-*N-acetyl*], [1-^{14}C-*N-acetyl*]	control	1.005 ± 0.005	1.003 ± 0.004	1.002 ± 0.010

[a] The isotope effects obtained with CMP-NeuAc and the isotope effects for solvolysis are included for comparison. [b] KIEs for solvolysis of CMP-NeuAc taken from ref *25*. [c] KIE for solvolysis of UMP-NeuAc, this work.

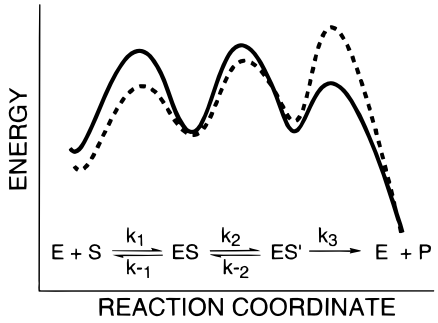

FIGURE 4: Qualitative comparison of the reaction coordinate for sialyltransferase-catalyzed transfer of CMP-NeuAc and UMP-NeuAc. The solid line corresponds to CMP-NeuAc, and the dashed line corresponds to UMP-NeuAc. For presentation, the binding of the acceptor substrate is not shown.

their identical structure at and around the atoms of the scissile glycosidic bond, and by the experimental observation that KIEs for solvolysis of each are identical. There must be a kinetically slow step after binding of CMP-NeuAc but before the irreversible chemical step to account for the difference in *V/K* isotope effects measured with UMP-NeuAc and CMP-NeuAc. This is presented in qualitative terms in Figure 4, which presents a minimal kinetic mechanism that can account for a *V/K* isotope effect that is sensitive to barriers for binding: an isomerization and an irreversible chemical step (glycosyl transfer). After binding to sialyltransferase (k_1), the CMP-NeuAc−enzyme complex can isomerize (k_2) and proceed further to form product or dissociate (k_{-1}) with equal probability ($k_{-1} = k_2$). From the isomerized state ES′, the CMP-NeuAc complex is more likely to proceed to product than it is to back-isomerize to the initial complex ($k_3 > k_{-2}$). It is this propensity that dramatically reduces the observed isotope effects with CMP-NeuAc as substrate. When UMP-NeuAc is the substrate, it is bound more weakly than CMP-NeuAc. In comparison, it is more likely to dissociate than it is to proceed in the forward direction ($k_{-1} > k_2$), and this reduces the external commitment to catalysis. UMP-NeuAc's reduced k_{cat} argues that the barrier for the glycosyl transfer step is higher than the barrier for CMP-NeuAc. So it is more likely to back-isomerize (and ultimately dissociate) than CMP-NeuAc. Possibly, the equilibrium for UMP-NeuAc in the ES and ES′ states may disfavor reaching the ES′ state. This amounts to an increase in k_{-2} which will contribute to lowering the internal commitment to catalysis.

A second and key observation was that solvent isotope effects are 0.97 ± 0.03 and 1.12 ± 0.19 for V_{max} and $V/K_{UMP-NeuAc}$ when UMP-NeuAc is the sialyl donor, but if CMP-NeuAc is used, the solvent deuterium isotope effect is 2.6 ± 0.3 on V_{max} and is 1.3 ± 0.1 on $V/K_{CMP-NeuAc}$. This interesting result shows that raising the barrier for the chemical step abolishes the solvent isotope effect, indicating that the step which is sensitive to the solvent isotope effect is not the step corresponding to glycosyl transfer. This step could be the proposed conformational change (i.e., step k_2 of Figure 4), but further work will be required to distinguish between this possibility and the possibility that the solvent effect on V_{max} is due to a step after cleavage of the glycosidic bond. Taken together, the results require a minimum of one additional kinetically slow step on the sialyltransferase catalytic cycle, and the fact that the solvent isotope effects are greatly diminished for the slow substrate UMP-NeuAc argues that proton transfer is not part of the transition state.

Features of Acid−Base Catalysis. A comparison of the pH−rate profiles in Figure 2 and Figure 3 provides a clear demonstration of how the use of UMP-NeuAc as the donor substrate has simplified the kinetic behavior of the enzyme. The profiles with UMP-NeuAc were well-fit to a bell-shaped profile for two ionizable groups, unlike the profiles with CMP-NeuAc which did not fit a simple bell model. The observed pK_a values with UMP-NeuAc are probably not obscured by kinetic features. The behavior of the k_{cat}/K_m data for UMP-NeuAc is consistent with sialyltransferase requiring two ionizable groups for catalysis with one pK_a of 6.2 and another pK_a of 8.9. Since UMP-NeuAc does not show any ionizations over this range, we attribute these ionizations to the free enzyme. Under V_{max} conditions, the ternary complex shows a downward shift of the acid-side pK_a from 6.2 to 5.5, and the alkaline pK_a is essentially unchanged at 9.0. Two reasonable functions for the protonated group would be for it to act as an acid to assist cleavage of the glycosidic link to the nucleotide, or it could provide a hydrogen in a critical hydrogen bond. Phosphate is a stable leaving group, so a requirement for protonating a phosphate to stabilize the transition state seems questionable. On the other hand, a proton donated to the exocyclic glycosidic oxygen would be expected to weaken the glycosidic bond and thus could provide a possible source of rate acceleration. Solvent isotope effects do not support a proton in flight in the transition state, and a pre-protonation of the exocyclic glycosidic oxygen would be extremely unfavorable on thermodynamic grounds given its very low basicity. The anionic nonbridging phosphate oxygen would be considerably easier to protonate, but it was not immediately obvious as to whether protonation here could help in catalysis. Theoretical calculations were used to help explore this question. Protonation of the nonbridging oxygen of the acetal phosphate model shown in Figure 5, right side, resulted in a decrease in the bond order of the glycosidic bond by 0.18. This would be a catalytic effect since the decreased bond order reflects a weakened C−O glycosidic bond. Protonation of the bridging glycosidic oxygen (Figure 5, left) also caused a decrease of

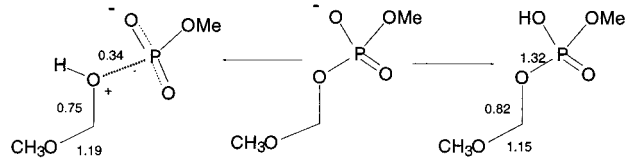

FIGURE 5: Effect of phosphate protonation state on acetal C−O bond order. For the sake of calculating the bond orders for the protonated structures, the bond orders in the middle structure were defined to be equal to 1. The calculations were performed with the 6-31G* basis set and density functional theory using the Becke exchange functional and the Lee−Yang−Parr correlation functional (*48*, *49*).

C−O glycosidic bond order, by 0.25, but the overwhelming effect was at the O−P bond which dramatically decreased by 0.66 in bond order. The calculations suggest that protonation of the bridging oxygen would favor phosphoryl transfer whereas protonation of the nonbridging phosphate oxygen favors glycosyl transfer. On this basis, we suggest that if sialyltransferase utilizes acid catalysis to facilitate loss of CMP, it may do so by protonating the nonbridging phosphate oxygen. Work is in progress to measure leaving group oxygen isotope effects to possibly locate the protonation site (*41*).

As mentioned above, the pH−rate profile with UMP-NeuAc was bell-shaped, and one possible interpretation of the acid-side ionization would be involvement of a general base. A commonly suggested chemical role would be to deprotonate the hydroxyl group of the acceptor oligosaccharide to facilitate its attack on the glycosidic carbon. In an associative displacement mechanism, the deprotonation would increase the nucleophilicity of the hydroxyl group, but it is difficult to imagine that deprotonation would be required for catalysis in a mechanism which is as dissociative as the sialyltransferase mechanism is. The barrier for capture of the sialyl oxocarbenium ion is extremely small (*27*, *28*) and should be one of the fastest steps in the reaction sequence. One way to reconcile the experimentally observed pH−rate dependence would be if the "basic" group serves to orient the acceptor hydroxyl group in a productive conformation. Alternatively, if the basic group is anionic, a possible function could be to help stabilize development of the cationic transition state. It is also possible that the "basic" residue does accept a proton in the transition state, but in a highly asynchronous manner where proton transfer considerably lags behind formation of the glycosidic bond. Future studies which utilize ^{18}O KIEs for the acceptor hydroxyl group may allow us to identify its protonation state at the transition state.

Structural Characteristics of the Transition State. Our working model for sialyltransferase catalysis starts with a pre-protonation of a nonbridging phosphate oxygen before cleavage of the glycosidic bond to CMP. The structure of the transition state that follows is identified on the basis of deuterium and ^{14}C KIEs (*42*). The β-dideuterium KIE of 1.218 ± 0.010 is nearly as large as the KIE for solvolysis of CMP- or UMP-NeuAc (Table 2). The solvolysis reaction transition state is purely dissociative, and by the comparable size of the KIEs, the sialyltransferase transition state must be similar. This is characteristic of a transition state with oxocarbenium ion character (*43*). The primary ^{14}C KIE of 1.028 ± 0.010 with UMP-NeuAc supports this explanation. This effect is in the range seen for dissociative type mechanisms, and is identical to the KIE measured for solvolysis of CMP-NeuAc (*25*, *44*). This small primary carbon KIE rules out significant nucleophilic participation in concert with loss of the UMP leaving group. The β-^2H KIEs show that the transition state for glycosidic bond cleavage has substantial positive charge. The lack of significant participation by the acceptor oligosaccharide would allow for the possibility that after the transition state a very short-lived oxocarbenium ion intermediate is formed; this is precedented for β-galactosidase (*45*). In solution, the NeuAc oxocarbenium ion species is very short-lived (*27*), so if it were generated in the active site, it is likely that it would be readily trapped by the acceptor in a kinetically invisible step. Another aspect of the transition state involves a binding interaction at C9 of the glycerol tail on the NeuAc residue. This follows from the substantial inverse ^3H isotope effect of 0.944 that indicates that the hydrogen at C9 is in a tighter vibrational environment in the transition state than in the ground state. It is not yet clear what specific molecular interactions are responsible for the isotope effect. The apparent binding and recognition of this side chain by sialyltransferase may be an important component of inhibitor design for sialyltransferases.

Directions for Inhibitor Design. Recently the first potent inhibitors of sialyltransferases were reported (*46*). These compounds linked a cytidine monophosphate moiety with groups that were planar and sought to mimic the presumed planar geometry of the oxocarbenium transition state that would arise in a dissociative type mechanism. The present studies confirm that the rat liver $\alpha(2\rightarrow 6)$ sialyltransferase has a transition state with nearly a full positive charge, indicating that cleavage of the CMP group is complete, or very nearly so. It will be of considerable interest to see if charge-mimic transition state analogues of the sialyl oxocarbenium ion (*47*) will prove to be useful inhibitors of sialyltransferase. Sialyltransferase must apparently undergo a conformational change prior to being competent for the glycosyl transfer step. Some evidence for this is found in the observation that while the enzyme can bind the donor substrate CMP-NeuAc, it does not hydrolyze it. It is when both substrates are bound that the presumed precatalytic conformational change occurs. Optimal inhibitors of sialyltransferase might be those which contain the structural features that promote the enzyme's ability to reach a conformation that reflects the catalytic form. It is from this state that transition state analogue inhibitors that mimic charge and shape will exert their greatest inhibitory potential.

ACKNOWLEDGMENT

We thank Dr. W. F. Vann of the NIH for the gift of an *E. coli* clone containing a CMP-NeuAc synthase expression plasmid.

REFERENCES

1. Lehninger, A. L., Nelson, D. L., and Cox, M. M. (1993) *Principles of Biochemistry*, Chapter 11, pp 308−320, Worth Publishers, New York.
2. Cordes, E. H., and Bull, H. G. (1974) *Chem. Rev. 74*, 581.
3. Sinnott, M. L. (1990) *Chem. Rev. 90*, 1171−1202.
4. Withers, S. G. (1995) *Pure Appl. Chem. 67*, 1673−1682.

5. Schauer, R. (1982) *Adv. Carbohydr. Chem. Biochem. 40*, 131−234.
6. Harduin-Lepers, A., Recchi, M.-A., and Delannoy, P. (1995) *Glycobiology 5*, 741−758.
7. Yamamoto, T., Nakashizuka, M., and Terada, I.(1998) *J. Biochem. 123*, 94−100
8. Gilbert, M., Cunningham, A. M., Watson, D. C., Martin, A., Richards, J. C., and Wakarchuk, W. W. (1997) *Eur. J. Biochem. 249*, 187−194.
9. Jackson, R. J., Hall, D. F., and Kerr, P. J. (1999) *J. Virol. 73*, 2376−2384.
10. Varki, A. (1993) *Glycobiology 3*, 97−130.
11. Lowe, J. B. (1994) in *Molecular Glycobiology* (Fukuda, M., and Hindsgaul, O., Eds.) pp 163−205, Oxford University Press, New York.
12. Schauer, R., Kelm, S., Reuter, G., Roggentin, P., and Shaw, L. (1995) in *Biology of the Sialic Acids* (Rosenberg, A., Ed.) pp 7−67, Plenum Press, New York.
13. Powell, L. D., and Varki, A. (1995) *J. Biol. Chem. 270*, 14243−14246.
14. Crocker, P. R., Kelm, S., Hartnell, A., Freeman, S., Nath, D., Vinson, M., and Mucklow, S. (1996) *Biochem. Soc. Trans. 24*, 150−156.
15. Weinstein, J., Souza-e-Silva, U., and Paulson, J. C. (1982) *J. Biol. Chem. 257*, 13835−13844.
16. Weinstein, J., Lee, E. U., McEntee, K., Lai, P., and Paulson, J. C. (1987) *J. Biol. Chem. 262*, 17735−17743.
17. Weinstein, J., Souza-e-Silva, U., and Paulson, J. C. (1982) *J. Biol. Chem. 257*, 13845−13853.
18. Hokke, C. H., Van derVen, J. G. M., Kamerling, J. P., and Vliegenthart, J. F. G. (1993) *Glycoconjugate J. 10*, 82−90.
19. Wlasichuk, K. B., Kashem, M. H., Nikrad, P. V., Bird, P., Jiang, C., and Venot, A. P. (1993) *J. Biol. Chem. 268*, 13971−13977.
20. Van Dorst, J. A. L. M., Tikkanen, J. M., Krezdorn, C. H., Streiff, M. B., Berger, E. G., Van Kuik, J. A., Kamerling, J. P., and Vliegenthart, J. F. G. (1996) *Eur. J. Biochem. 242*, 674−681.
21. Higa, H. H., Paulson, J. C., and Weinstein, J. (1985) *J. Biol. Chem. 260*, 8838−8849.
22. Gross, H. J., Rose, U., Krause, J. M., Paulson, J. C., Schmid, K., Feeney, R. E., and Brossmer, R. (1989) *Biochemistry 28*, 7386−7392.
23. Kleineidam, R. G., Schmelter, T., Schwartz, R. T., and Schauer, R. (1997) *Glycoconjugate J. 14*, 57−66.
24. Comb, D. G., Watson, D. R., and Roseman, S. J. (1966) *J. Biol. Chem. 241*, 5637−5642.
25. Horenstein, B. A., and Bruner, M. (1996) *J. Am. Chem. Soc. 118*, 10371−10379.
26. Horenstein, B. A. (1997) *J. Am. Chem. Soc. 119*, 1101−1107.
27. Horenstein, B. A., and Bruner, M. (1998) *J. Am. Chem. Soc. 120*, 1357−1362.
28. Horenstein, B. A. (1999) in *Transition-state Modeling for Catalysis*, ACS Symp. Ser. #721 (Truhlar, D. G., and Morokuma, K., Eds.) American Chemical Society, Washington, DC.
29. Bruner, M., and Horenstein, B. A. (1998) *Biochemistry 37*, 289−297.
30. Liu, J. L., Shen, G.-J., Ichikawa, Y., Rutan, J. F., Zapata, G., Vann, W. F., and Wong C.-H. (1992) *J. Am. Chem. Soc. 114*, 3901−3910.
31. Dalquist, F. W., Rand-Meir, T., and Raftery, M. A. (1969) *Biochemistry 8*, 4214−4221.
32. Parkin, D. L. (1991) in *Enzyme Mechanisms from Isotope Effects* (Cook, P. F., Ed.) pp 269−290, CRC Press, Boca Raton, FL.
33. Duggleby, R. G., and Northrop, D. B. (1989) *Bioorg. Chem. 17*, 177−193.
34. Bigeleisen, J., and Wolfsberg, M. (1958) *Adv. Phys. Chem. 1*, 15−76.
35. Salomaa, P., Schaleger, L. L., and Long, F. A. (1964) *J. Am. Chem. Soc. 86*, 1−7.
36. Kirshenbaum, I. (1951) *Physical Properties and Analysis of Heavy Water*, p 33, McGraw-Hill, New York.
37. Miner, C. S., and Dalton, N. N. (1953) *Glycerol*, ACS Monograph Series, pp 240−241, Reinhold Publishing Corp., New York.
38. Simon, H., and Palm, D. (1966) *Angew. Chem., Int. Ed. Engl. 5*, 920−933.
39. Northrop, D. B. (1977) in *Isotope Effects on Enzyme Catalyzed Reactions* (Cleland, W. W., O'Leary, M. H., and Northrop, D. B., Eds.) University Park Press, Baltimore.
40. Cleland, W. W. (1982) *CRC Crit. Rev. Biochem. 13*, 385−427.
41. Bruner, M., and Horenstein, B. A., unpublished results.
42. Schramm, V. L. (1991) in *Enzyme Mechanisms from Isotope Effects* (Cook, P. F., Ed.) CRC Press, Boca Raton, FL.
43. Melander, L., and Saunders, W. H. (1980) *Reaction Rates of Isotopic Molecules*, Chapter 6, Kreiger, Malabar, FL.
44. Goiten, R. K., Chelsky, D., and Parsons, S. M. (1978) *J. Biol. Chem. 253*, 2963−2971. Bennett, A. J., and Sinnott, M. L. (1986) *J. Am. Chem. Soc. 108*, 7287−7294. Melander, L., and Saunders, W. H. (1980) in *Reaction Rates of Isotopic Molecules*, pp 242−246, Kreiger, Malabar, FL.
45. Richard, J. P., Huber, R. E., Heo, C., Amyes, T. L., and Lin, S. (1996) *Biochemistry 35*, 12387−12401.
46. Muller, B., Schaub, C., and Schmidt, R. R. (1998) *Angew. Chem., Int. Ed. Engl. 37*, 2893−2897.
47. Parr, I. B., and Horenstein, B. A. (1997) *J. Org. Chem. 62*, 7489−7494.
48. Becke, A. D. (1993) *J. Chem. Phys. 98*, 5648−5652.
49. Lee, C., Yang, W., and Parr, R. G. (1988) *Phys. Rev. B 37*, 785−789.

BI991474H